



Supplement of

**Significant concentrations of nitryl chloride sustained in the morning:
investigations of the causes and impacts on ozone production in a polluted
region of northern China**

Yee Jun Tham et al.

Correspondence to: Tao Wang (cetwang@polyu.edu.hk)

The copyright of individual parts of the supplement might differ from the CC-BY 3.0 licence.

Table S1. Validation of meteorological simulations by WRF.

	T (°C)	RH (%)	WD (°)	WS (m/s)
Observation Average	24.00	74.31	161.03	1.75
Simulation Average	23.03	78.03	162.76	2.15
mean bias	-0.96	3.72	1.72	0.39
root mean square error	2.70	10.67	122.26	1.54

5

Table S2. Mean concentrations and standard deviations (σ) of each species and meteorological conditions used as input in the box-model simulations. Concentrations are in ppbv unless stated.

Species	Average		Megacity case	
	Mean	$\pm \sigma$	Mean	$\pm \sigma$
ClNO ₂	0.19	0.16	0.52	0.65
NO	1.32	1.30	0.65	0.76
NO ₂	13.11	5.96	10.37	5.28
O ₃	54.3	30.2	54.6	29.1
SO ₂	6.75	3.51	4.373	4.18
CO	549	63	541	207
HONO	0.75	0.37	0.51	0.29
HCl	1.15	0.40	1.26	0.93
methane	2361	362	2090	233
methanol	24.707	5.673	15.698	4.805
acetaldehyde	1.887	0.357	1.349	0.383
acetic acid	5.013	0.897	2.437	0.610
acetone	4.796	0.583	3.345	0.353
formaldehyde	7.247	1.394	3.475	0.545
ethane	2.950	0.454	2.465	0.717
ethene	1.813	0.860	1.034	0.721
propane	1.171	0.304	1.186	0.456
propene	0.310	0.170	0.221	0.161
i-butane	0.413	0.130	0.359	0.159
n-butane	0.701	0.249	0.591	0.292
ethyne	1.490	0.282	0.835	0.267

1-butene	0.031	0.017	0.038	0.036
2-methylpropene	0.063	0.034	0.032	0.035
trans-2-butene	0.177	0.027	0.062	0.023
cis-2-butene	0.015	0.006	0.011	0.011
i-pentane	0.411	0.141	0.310	0.181
n-pentane	0.322	0.124	0.204	0.129
1,3-butadiene	0.022	0.016	0.014	0.012
1-pentene	0.017	0.008	0.016	0.009
isoprene	0.664	0.473	0.249	0.237
2,3-dimethylbutane	0.090	0.029	0.062	0.022
2-methylpentane	0.154	0.055	0.144	0.086
MTBE	0.121	0.045	0.073	0.048
3-methylpentane	0.119	0.047	0.086	0.054
1-hexene	0.056	0.021	0.044	0.017
n-hexane	0.148	0.064	0.120	0.085
methyleneethylketone	2.004	0.106	3.401	0.562
2-methylhexane	0.033	0.012	0.028	0.017
cyclohexane	0.051	0.022	0.042	0.027
3-methylhexane	0.056	0.019	0.044	0.022
benzene	1.007	0.265	0.592	0.229
n-heptane	0.080	0.025	0.061	0.037
toluene	0.786	0.273	0.566	0.291
n-octane	0.054	0.014	0.029	0.020
ethylbenzene	0.198	0.066	0.160	0.089
n-nonane	0.028	0.010	0.019	0.012
o-xylene	0.097	0.036	0.069	0.034
styrene	0.047	0.030	0.033	0.026
m-ethyltoluene	0.021	0.008	0.019	0.010
1,3,5-trimethylbenzene	0.019	0.006	0.019	0.008
1,2,4-trimethylbenzene	0.095	0.027	0.058	0.025
1,2,3-trimethylbenzene	0.017	0.005	0.016	0.006
Aerosol surface area ($\mu\text{m}^2 \text{ m}^{-3}$)	1.60×10^{-3}	3.72×10^{-4}	1.24×10^{-3}	4.92×10^{-4}
Temperature (K)	300.00	3.12	296.49	3.56
Relative Humidity (%)	64	12	67	17
$j_{\text{NO}_2} (\text{s}^{-1})^a$	3.16×10^{-3}	2.01×10^{-3}	3.33×10^{-3}	2.52×10^{-3}
$j_{\text{O}_3(\text{O}^1\text{D})} (\text{s}^{-1})^a$	7.25×10^{-6}	6.36×10^{-6}	7.33×10^{-6}	6.99×10^{-6}
$j_{\text{HONO}} (\text{s}^{-1})^a$	5.38×10^{-4}	3.45×10^{-4}	5.68×10^{-4}	4.29×10^{-4}
$j_{\text{CINO}_2} (\text{s}^{-1})^a$	1.27×10^{-4}	8.06×10^{-5}	1.53×10^{-4}	1.26×10^{-4}

^a from sunrise to sunset

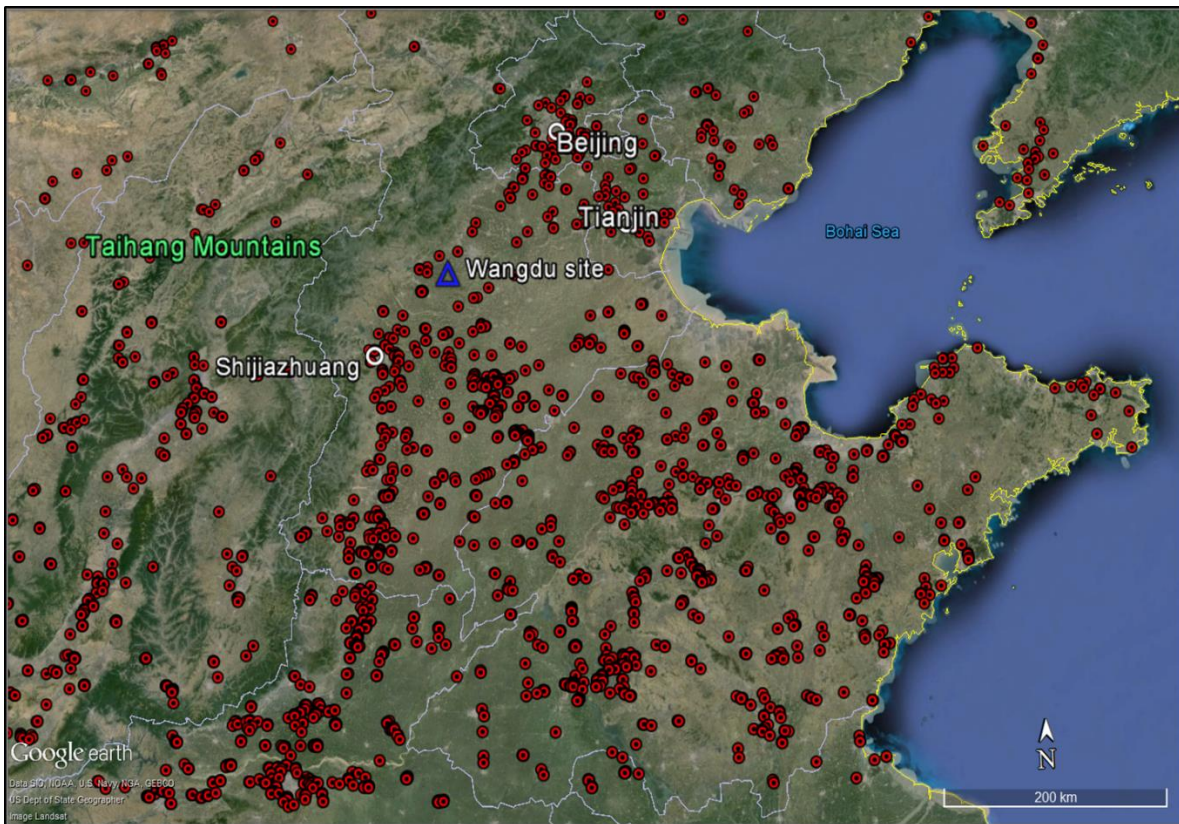


Figure S1. Active fire hotspots (red dots) in NCP from FIRMS covering the study period of 20 June – 9 July 2014 (Data available at <https://earthdata.nasa.gov/firms>).

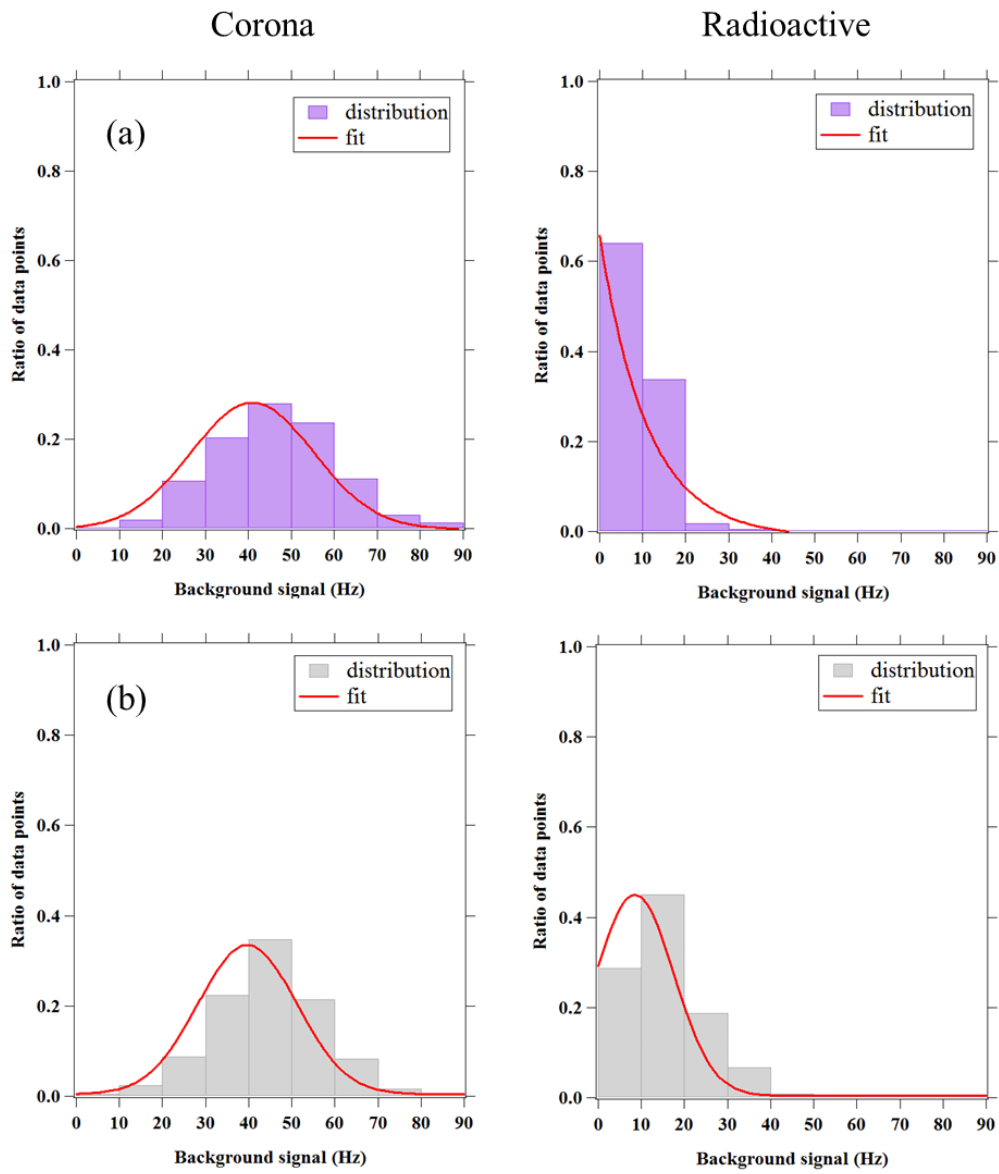


Figure S2. Distributions of ambient background signals of ClNO₂ (in purple) and N₂O₅ (in grey) from CIMS operated with corona discharge source and ²¹⁰Po radioactive source ($N = 902$).

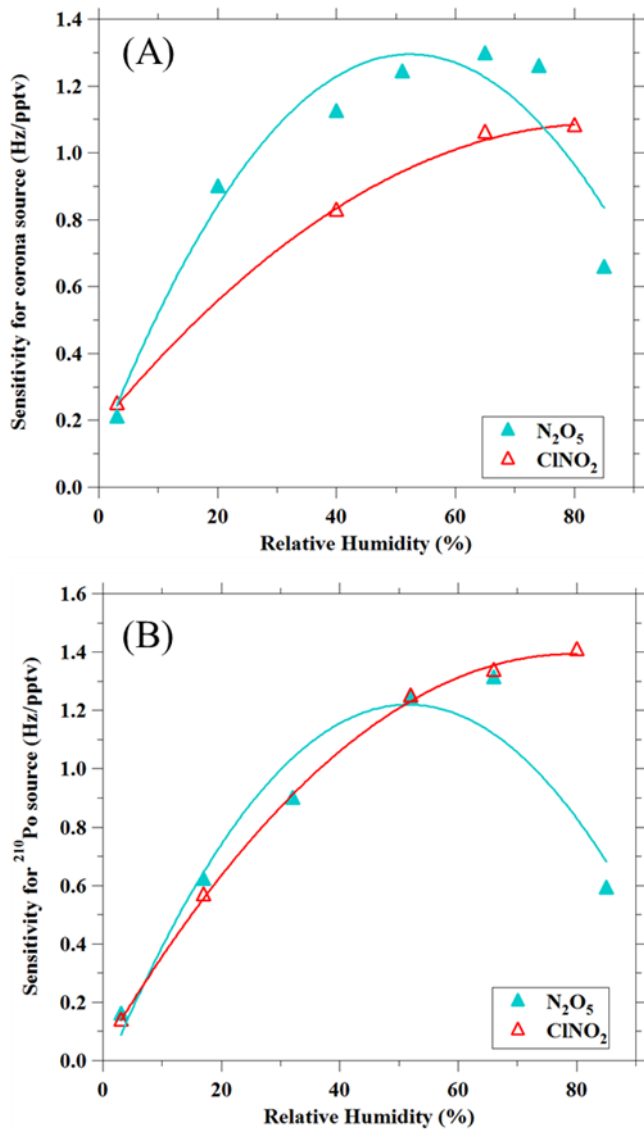


Figure S3. An example of sensitivity for N_2O_5 and ClNO_2 against the relative humidity when (a) corona discharge and (b) ^{210}Po were used. The solid line represents the curve fits of the data.

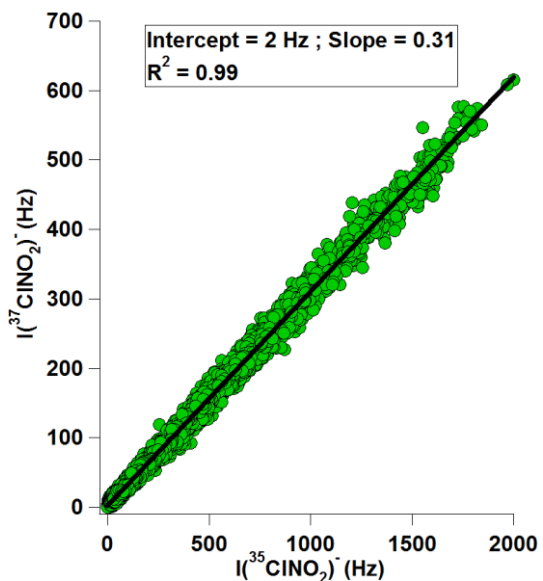


Figure S4. Scatter plot of 210 m/z against the 208 m/z.

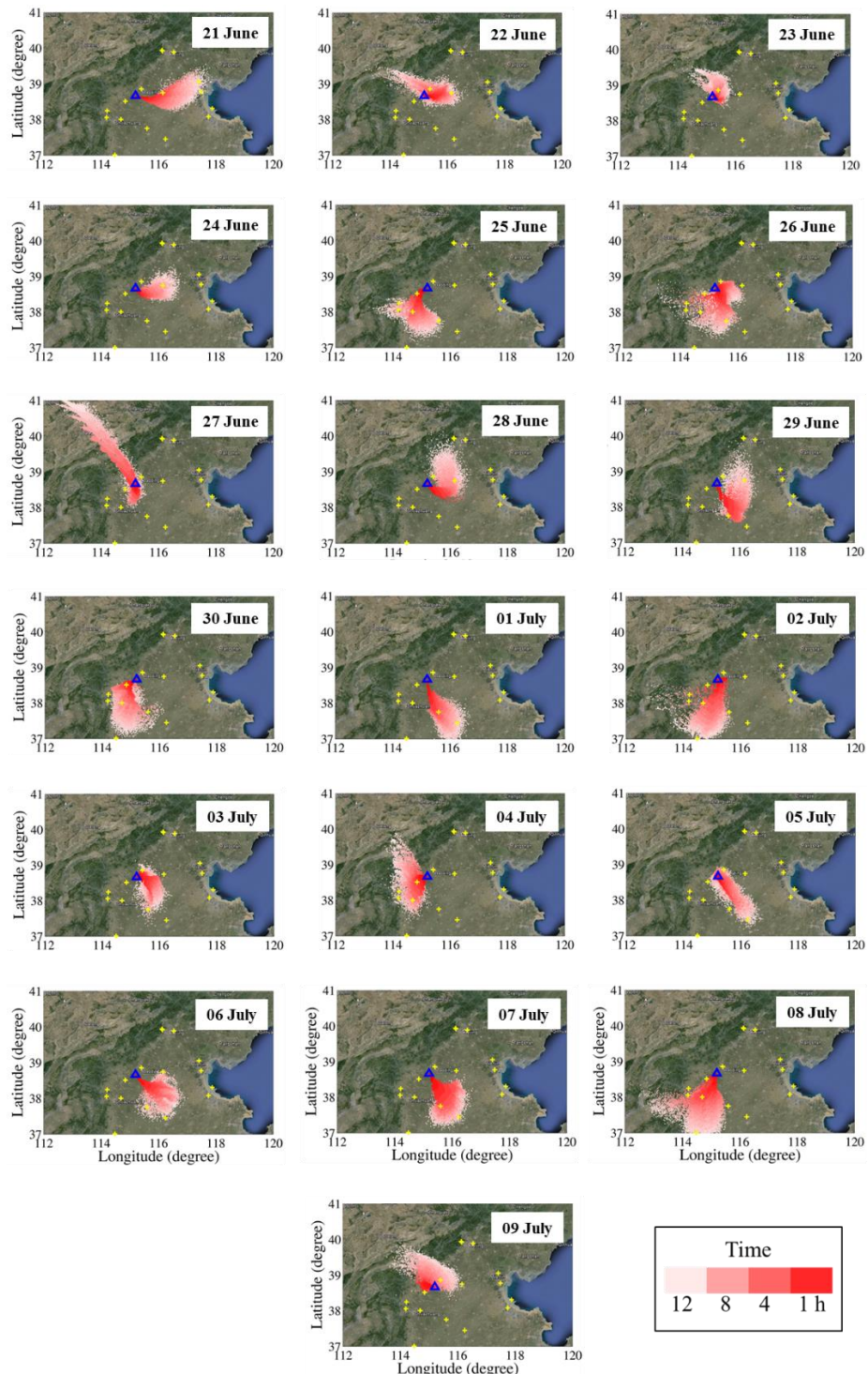


Figure S5. History of air masses that arrived Wangdu sampling site at 00:00.

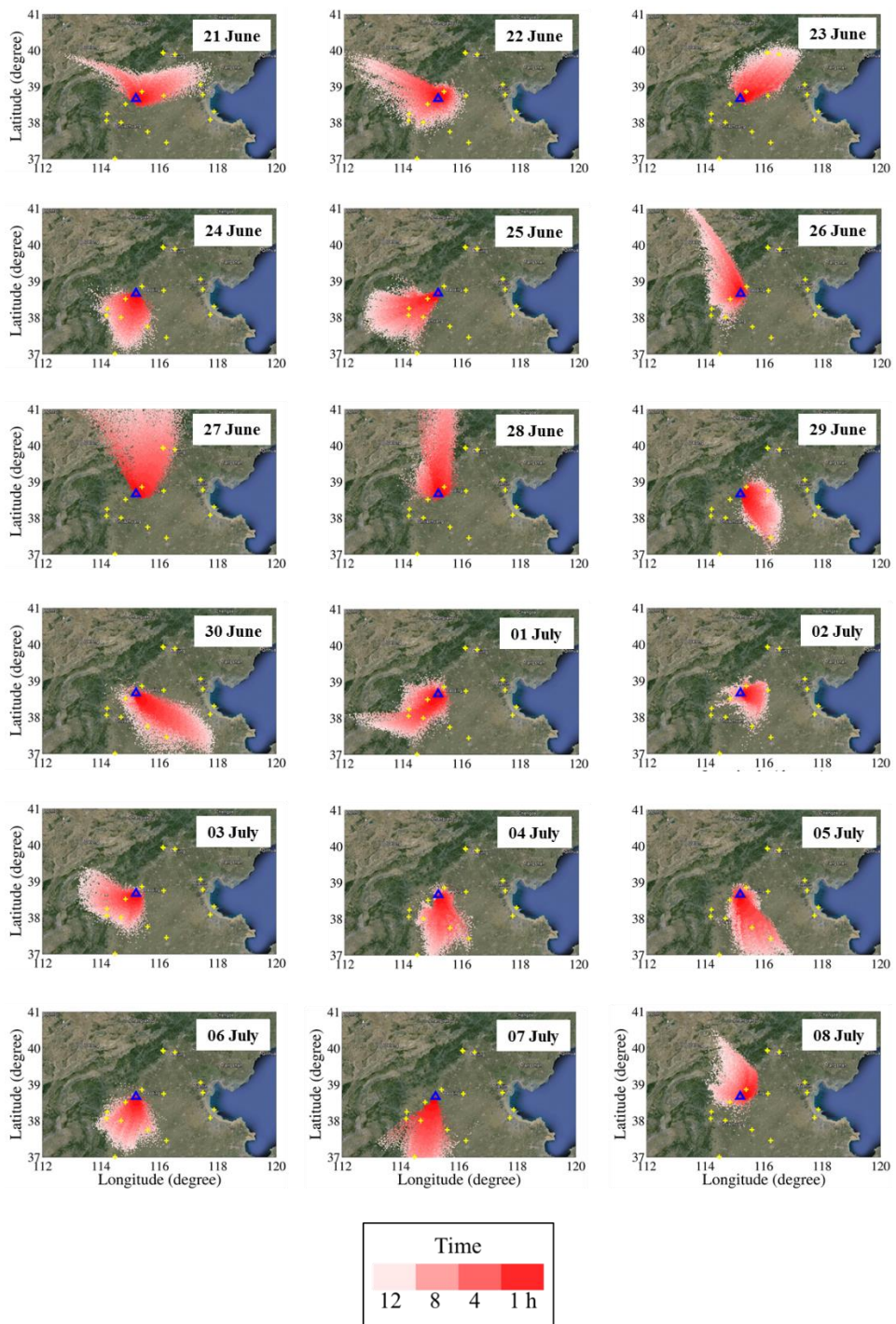


Figure S6. History of air masses that arrived Wangdu sampling site at 14:00.

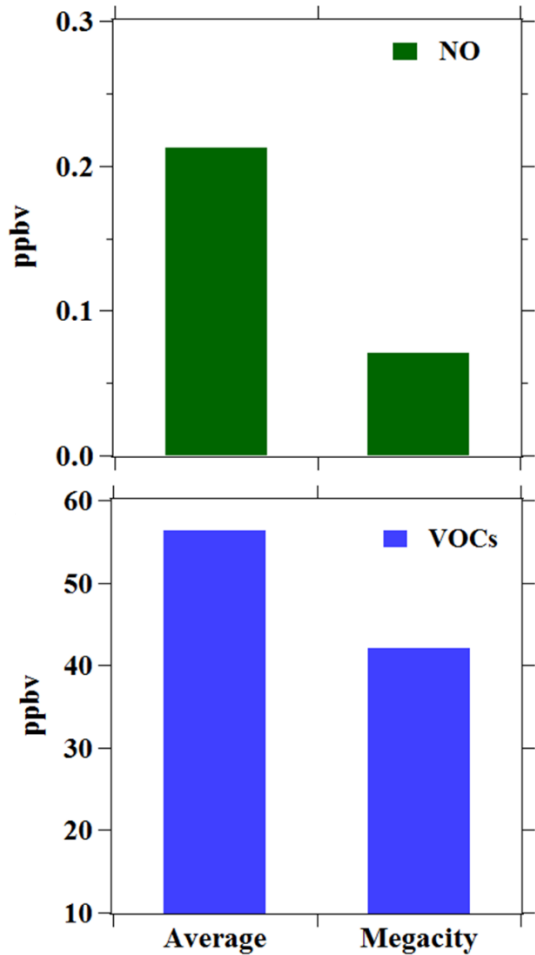


Figure S7. Different level of NO (upper) and total VOCs (lower) between campaign average and the megacity case (averaged between 20:30 to 23:30 of the night).

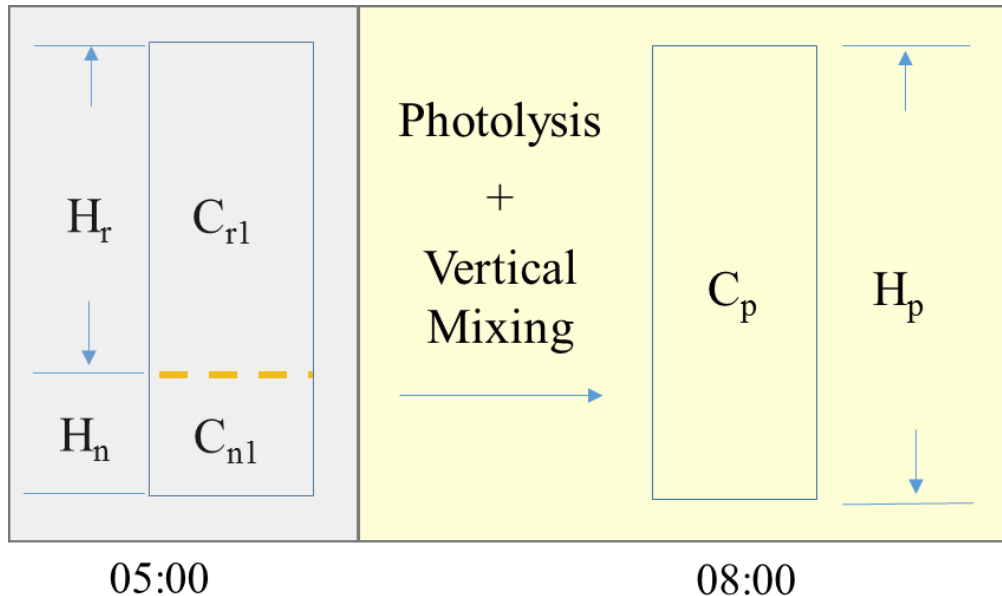


Figure S8. Conceptual diagram of 1-D model used for the estimation of CINO₂ mixing ratios in the RL before sunrise.

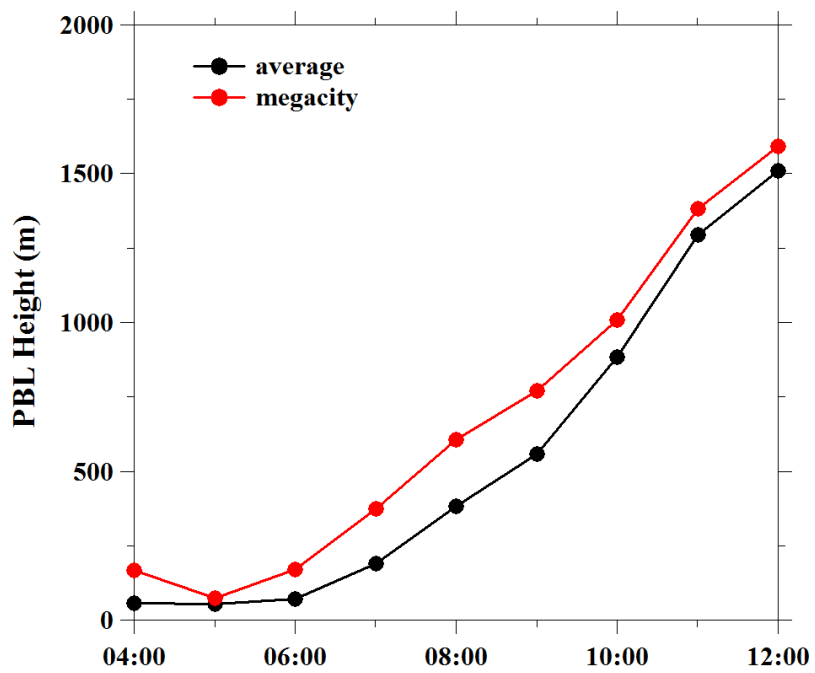
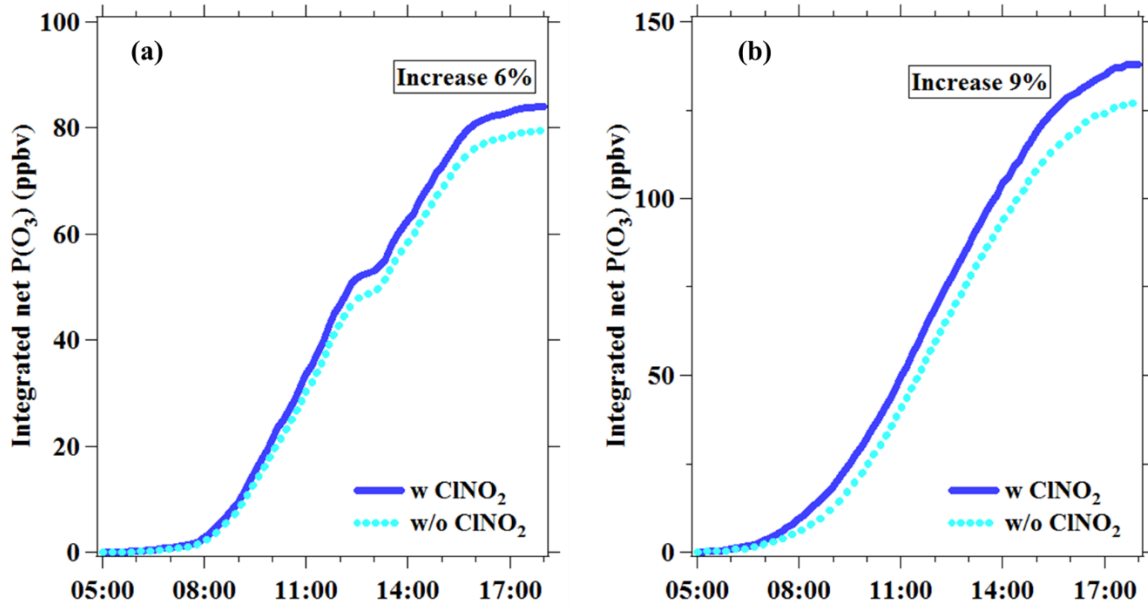


Figure S9. WRF simulated PBL heights (a.g.l.) for the campaign average and the megacity case.



5 **Figure S10.** Daily integrated net O_3 production simulated with and without ClNO_2 input; (a) the ClNO_2 concentration in megacity case was decreased similar to that of average condition, and b) the ClNO_2 concentration in average condition was increased to that of megacity case.

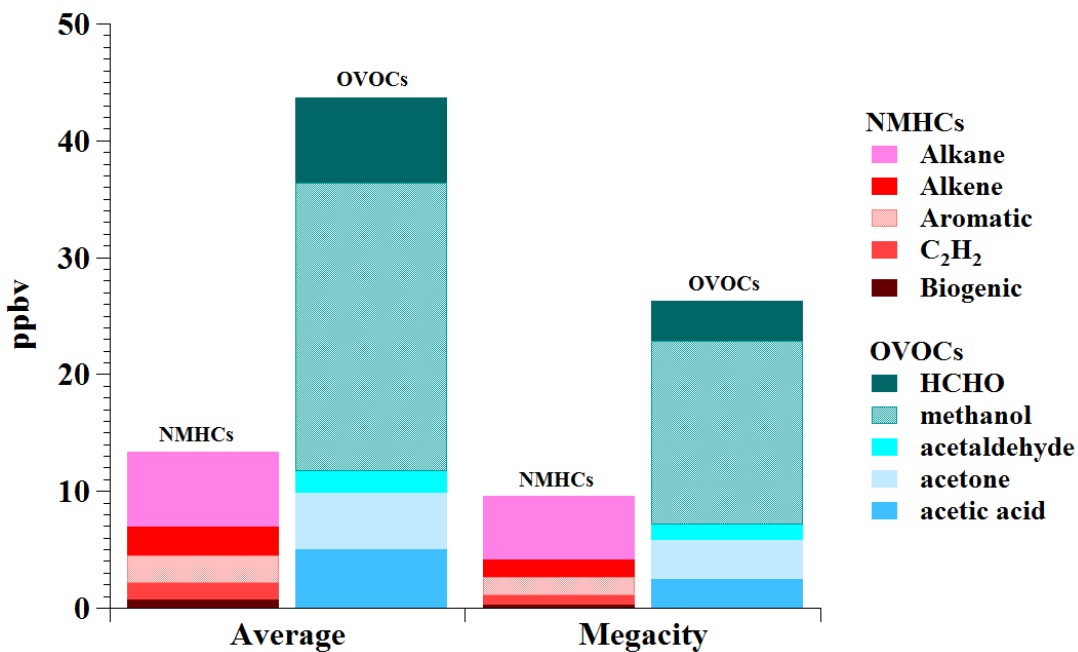


Figure S11. 24-hour average concentrations of different NMHCs and OVOCs groups/species for campaign average and the megacity case.

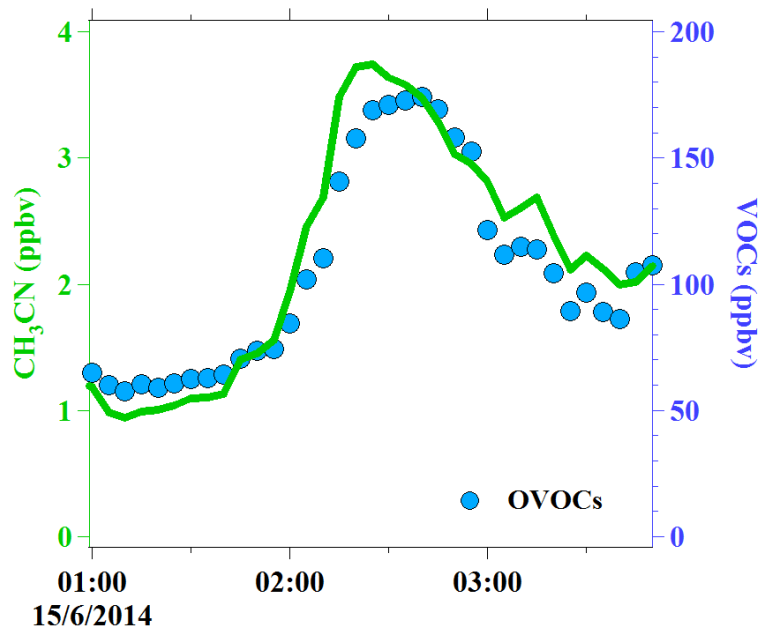


Figure S12. Huge amount of OVOC observed in a fresh biomass burning plume in early morning of 15 June 2014 (as indicated by high CH₃CN).

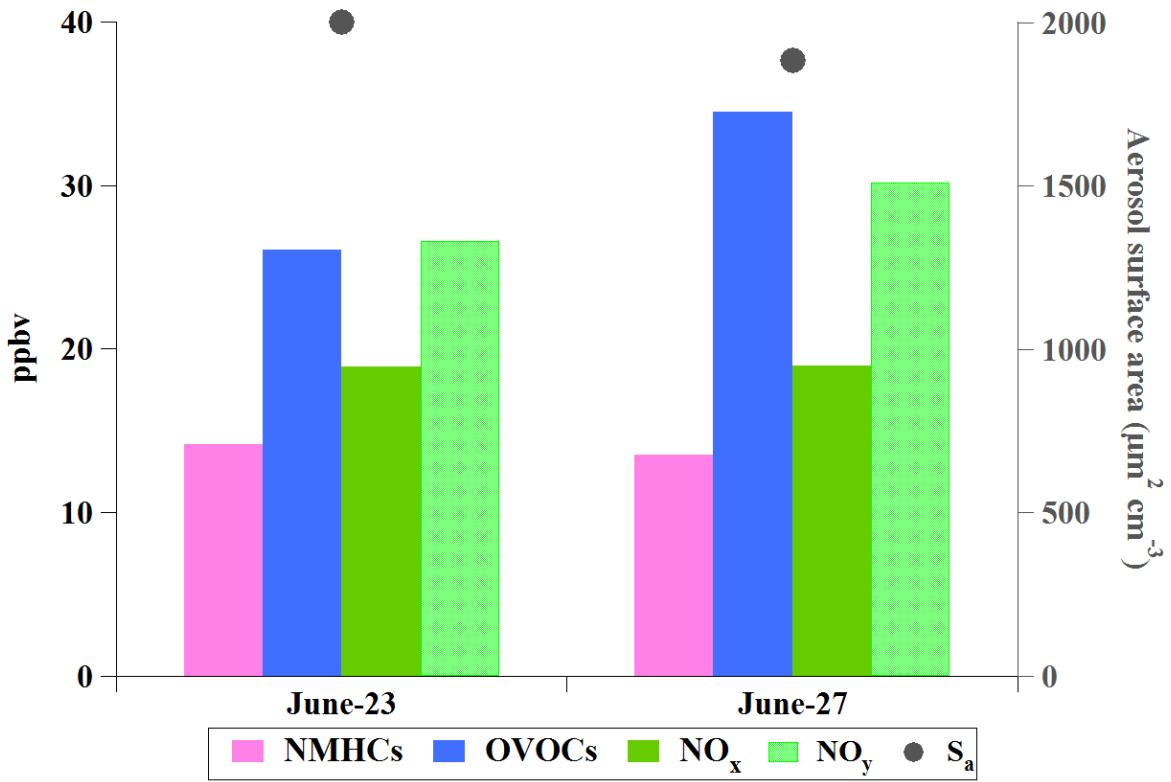


Figure S13. Examples of smaller OVOC to NMHC ratios and similar mean mixing ratio of NO_x , NO_y , and S_a in other cases of megacity outflow from Beijing/Tianjin on 23 and 27 June 2014.